NASA Technical Memorandum 79308

RESULTS OF DUCT AREA RATIO CHANGES IN THE NASA LEWIS H_2-O_2 COMBUSTION MHD EXPERIMENT

J. Marlin Smith
Lewis Research Center
Cleveland, Ohio

RESULTS OF DUCT AREA RATIO CHANGES IN THE
NASA LEWIS H_2-O_2 COMBUSTION MHD EXPERIMENT

J. Marlin Smith
NASA Lewis Research Center
Cleveland, Ohio 44135

Abstract

MHD power generation experiments utilizing a cesium-seeded H_2-O_2 working fluid have been carried out using a diverging area Hall duct having an entrance Mach number of 2. The experiments are conducted in a high-field strength cryomagnet facility at field strengths up to 5 tesla. The effects of power takeoff location, generator loading, B-field strength, and electrode breakdown voltage have been investigated. In this paper the effect of area ratio, multiple loading of the duct, and duct location within the magnetic field are considered.

I. Introduction

The Lewis Research Center (LeRC) has in operation a small (4-12 MW$_T$) cesium-seeded H_2-O_2 combustion MHD generator to investigate performance and fluid dynamics at high magnetic field levels. The MHD power generation experiments are conducted in a high magnetic field strength cryomagnet facility. While this facility has the capability to produce fields > 6 tesla, the peak field utilized to date is 5 tesla. In the initial experiments, the Hall generator configuration was chosen for its simplicity of construction and is designed to operate supersonically (Mach 2 at entrance) over a range of combustion pressures (5-20 atm) and a range of oxygen/fuel weight ratios (4-12). This facility and the associated MHD hardware are discussed in Section II.

In our initial experiments (reference 1), a conically bored duct with an overall area ratio of 2.56 was used. The effects of power takeoff location, generator loading, B-field strength, and electrode breakdown voltage were investigated. As a result of these experiments and subsequent theoretical analysis, it was established that a further increase in performance could be achieved with a duct of larger area ratio, by multiple loading the duct, and by relocating the duct within the magnetic field. For the present experiment the duct was bored to an area ratio of 4. The effect of this increased area ratio, multiple loading, and new duct location within the magnetic field are discussed in Section III.

II. Experimental Facility

The MHD power generation experiments are conducted in a high-field strength cryomagnet (fig. 1) which was adapted from an existing facility. In its original construction, it consisted of 12 high purity aluminum coils which are pool cooled in a bath of liquid neon. In this configuration, a peak field of 15 tesla was produced. For the present experiments, the center four coils were removed and a 23 cm diameter transverse warm bore tube was inserted to allow the placement of the MHD experiment between the remaining eight coils as shown in the cross section insert in figure 1. In this configuration, a peak field of > 6 tesla should be obtainable. The time duration of the experiment is limited by the neon supply which allows on the order of one minute of total operating time followed by an 18-hour reliquefaction period. As a result, the experiments are run in a pulsed mode. The run duration for the data presented here was 5 sec.

In the rocket engine modified for use in this program, the gaseous H_2 is injected uniformally into the combustion chamber through a porous stainless steel injection plate at the rear of the chamber. The gaseous O_2 is injected through 36 injection tubes uniformally inserted into the H_2 injection plate. Cesium seed is injected into the oxygen supply line as a 75 percent solution by weight of CSOH dissolved in water. The combustion cl.amber and nozzle are water-cooled electrodeposited copper capable of steady-state operation. The length of the chamber and nozzle is 22.86 cm and the i.d. for the chamber is 6.35 cm. The nozzle is designed for Mach 2 at the 4.96 cm diameter exit. The engine is capable of operation at stagnation pressures between 5 and 20 atm and at O/F weight ratios from 4-12.

Experiments have been carried out using a diverging circular cross section duct having an inlet Mach number 2. In our initial experiments (reference 1) the duct had an exit to inlet area ratio, AR, of 2.56. In the present experiments the area ratio is 4. The heat sink duct is constructed from 42 cooper electrodes, 1.27 cm wide and electrically insulated from one another by a high-temperature asbestos sheet (to provide pressure seal), sandwiched between two sheets of

mica (to provide electrical insulation). The duct (figure 2) is built up in modular form, each module consisting of 8-15.24 cm o.d. rings clamped together between two triangular shaped pieces by three electrically insulated stainless steel bolts. Lateral movement of the rings is negated by three fiberglas rods inserted through the entire module. Four such modules are used in the present experiments with 2.54 cm end flanges for a total of 42 electrodes. Figure 2 is a picture of the combustor-generator-diffuser assembly.

The entire combustor-generator-diffuser assembly is inserted in the bore tube as shown   figure 1. The high-temperature exhaust gases are water quenched at the exit of the diffuser. The resulting water then passes back to a sump for recirculation. The water is periodically brought back to normal PH by acid addition after which it can be discarded through storm sewers.

While the facility is capable of being run over a wide range of parameters, the data which will be discussed in this report was taken for the following nominal conditions:

Combustion stagnation pressure	10 atm
Mass flow rate	.5 kg/sec
Seed fraction = $\frac{\text{wt. of Cs}}{\text{tot. wt.}}$	.05
Equivalence ratio	1.0
Thermal input	7 MW
Peak magnetic field	5 tesla
Entrance Mach number	2
Duct Entrance diameter	5.0 cm
Duct exit diameter	
2.56 AR duct	8.0 cm
4.00 AR duct	10.0 cm
Length of duct	58 cm

III. Experimental Results

Effect of Power Takeoff Location, Multiple Loading, Axial Duct Location

In these initial experiments, the Hall generator configuration was chosen over the more efficient Faraday or diagonal wall configurations due to its simplicity of construction. One advantage of the Hall and DW configurations over that of the Faraday is that power can be extracted by a single electrical load rather than requiring separate loads for each electrode. However, this can be a disadvantage since as the gas properties (particularly the electrical conductivity) change down the channel, the axially varying local internal impedance cannot be matched by the single external impedance.

The result of this is shown in figure 3 for the 2.56 AR duct. In this figure the generated voltage is plotted as a function of distance down the channel, i.e., electrode number. In Run 407, the external load (11.5Ω) was placed between the first three and the last three electrodes. It is seen that the voltage gradient between the third and twelfth electrode is negative indicating that power is being dissipated in this region. This is due to the

fact that insufficient voltage is being generated in this region to pass the current generated by the generator as a whole.

By eliminating this region from the load, i.e., moving the front power takeoff from electrodes 1-3 to electrodes 10-16, the power output was increased from 8.74 KW in Run 407 to 11.2 KW in Run 413. In the experimental data to be discussed for the 2.56 AR duct, the power akeoff electrodes were 11-13 and 40-42. It should also be noted from figure 3, that in run 413 the voltage gradient betweeen electrodes 1-10 is now positive, and hence additional power could be obtained from this region by loading with an appropriately matched impedance. The effect of multiple loading will be discussed later in this section.

When the 4 AR duct was loaded from the first three to the last three electrodes the region of negative power generation moved downstream to approximately the 15th electrode as compared to the 12th electrode as observed in the 2.56 AR duct. This resulted from the increased overall performance of the 4 AR duct and the fact that the increased area ratio was achieved by conically boring the duct from a fixed inlet area. Therefore increased performance was achieved in the downstream portion of the channel with little performance change upstream. As a result a greater portion of the upstream region of the duct was unable to support the increased performance of the duct as a whole so that maximum power output is achieved by excluding this region from the load. Unless otherwise noted the experimental data to be discussed for the 4 AR duct was obtained with the power takeoff electrodes connected from 14-16 to 40-42.

Although maximum power with a single load is extracted from the region of electrodes 14-16 to 40-42, the upstream region in this configuration (electrodes 1-14) generates a positive open circuit voltage (as in the 2.56 AR duct, see run 413 of figure 3) and hence could be used to generate power by separately loading this region. It was therefore of interest to see if indeed additional power could be generated in this manner and also to see if this affected power production in the downstream region.

In figure 4 the output voltage as a function of electrode number is shown for the optimum configuration for the multiple load case. In this case electrodes 6-15 were connected through a 10 Ω load while electrodes 15-42 were connected through a 12 Ω load. As in the single load case in which the load was across the entire duct, a region of negative power generation was found to exist in the region from electrodes 1 6 when the front end load was connected from electrodes 1-15. Therefore maximum power was obtained by excluding this region from the load. However, as can be seen from figure 4, the region possesses a positive open circuit voltage and additional power could be extracted by separately loading this region.

In the case of our small experiment, properties do not change significantly over the power generation region and hence the majority of the power (95%) can be extracted from a single load. However, in large ducts where a substantial fraction of the input power is extracted, the properties will vary significantly, and optimum performance will require multiple loading. Since the power output of the upstream region was small, no measureable effect upon the power generation in the downstream region could be detected.

Also to be noted from figures 3 and 4 is that the generated voltage at the end of the duct is still rising on a positive slope. This indicates that the magnetic field is still of sufficient strength beyond the end of the duct to allow additional power production. In order to investigate this possibility, tests were run with the duct moved downstream relative to the centerline of the magnet. The results are shown in figure 5. In this figure the magnetic field profile is shown in relation to the various duct locations. The axial voltage profiles as a function of distance from the magnet centerline are shown for the duct load resistance connected from electrodes 1-3 to 40-42. The curve labeled run 708 was the location of both the 2.56 AR and the 4 AR ducts during the tests discussed throughout the rest of the paper. Figure 5 shows that the effect of moving the duct downstream is to decrease the region of negative power generation in the front of the duct. However, as the duct is moved further downstream the magnetic field at the end of the generator finally becomes too small to generate sufficient voltage to maintain the current generated by the duct as a whole. As a result a region of negative power generation is produced at the end of the duct which decreases the power output. Therefore there is an optimal location for the present duct within the magnetic field which is approximately that of run 1012.

As a result of the loading and duct location tests discussed in this section, it can be concluded that a more optimal utilization of the magnetic field could be obtained with a longer duct. This would allow the use of the full extent of the downstream magnetic field while the upstream region of negative power generation could be made power producing by separately loading the front and rear regions of the duct with a common junction point at the inflection point of the voltage versus distance curve.

Power Output

In figure 6 the effect of B-field on the power generated is shown for the 2.56 AR and 4 AR ducts operating at a combustion pressure of 10 atm. It is seen that in both cases the power increases almost linearly with B^2. This dependency for a Hall generator at low Hall parameter (~ 1) was not expected. This B^2 dependency which is probably unique to our operating conditions and experiment. The maximum power output achieved for the 2.56 AR and 4 AR ducts was 87.5 KW and 153 KW, respectively.

Tests in the 2.56 AR duct were carried out over a pressure range of 5 to 13 atm. While the testing was not extensive at other than 10 atm, no shocks were observed within the duct. In the 4 AR duct a shock was observed in the duct even without power extraction for pressures at and below approximately 7 atm. The influence of B-field (power extraction) upon the location of the shock within the duct is shown in figure 7. It is seen that the shock moves upstream with increased B-field (power extraction). This has a profound influence upon the power that can be extracted from the channel, since in the region downstream of the shock the flow is subsonic and the reduced velocity results in a decrease in generated voltage. This is shown in figure 8 where the power output is plotted versus the square of the B-field. It is seen that while the power output still increases with B-field that the previously observed linear dependence at a combustion pressure of 10 atm no longer exists at a combustion pressure of 7 atm, and that the rate of power increase falls rapidly with increased B-field.

In figure 9 the power density as a function of distance down the channel is plotted for the 2.56 AR and 4 AR ducts at a B-field strength of 5 tesla and a combustion pressure of 10 atm. These curves were obtained by differentiating the measured Hall voltage profiles to obtain the local Hall electric field and by assuming that the measured Hall current completely and uniformly fills the duct cross sectional area so that the local current density could be obtained by dividing the measured current by the area. As can be seen from figure 9 the peak power density is substantially increased in the 4 AR duct as compared to the 2.56 AR duct being 110 MW/M^3 and 85 MW/M^3 respectively.

Voltage Breakdown

During the testing of the 2.56 AR duct, the question of interelectrode breakdown was extensively analyzed to determine if the H_2-O_2 combustion system would be limited by the same breakdown voltage as widely observed in other combustion MHD experiments, i.e., approximately 40 volts/insulator. In figure 10, the open circuit Hall voltage is plotted versus the square of the magnetic field. During the duration of our 5 second runs, no breakdown is observed below an average field of approximately 50 volts/insulator. Above this value the voltage still continues to increase with B^2. However, approximately 2.5 seconds after initiation of seed injection, breakdown occurs. After breakdown, a steady average voltage of approximately 40 volts/insulator is observed independent of magnetic field strength.

Upon disassembly of the channel, grooves approximately one-sixteenth of an inch wide perpendicular to the magnetic field were found to exist on the interelectrode insulators on the anode side of the channel. The damage was typical of the insulator shown in the upper left-hand corner of figure 11. The severity of the damage to the insulators (as measured by the length of the grooves) very nearly correlated to the power density profile shown in figure 8.

3

This effect was also observed in reference 1 and is due to the $\underline{jxB}$ force acting on the anode current tending to force it into the insulators.

Breakdown tests on the 4 AR channel have not as yet been performed. However, the peak voltage gradient achieved from the test results shown in figure 4 was 65 volts/insulator. In this test and others of similar electrical stress in the 4 AR duct, nc interelectrode breakdown has been observed.

IV. Concluding Remarks

In previous experiments (reference 1), performed in a conically bored duct with an overall area ratio of 2.56, the effects of power takeoff location, generator loading, B-field strength, and electrode breakdown voltage were investigated. As a result of these experiments, it was concluded that a further increase in performance could be achieved by increasing the area ratio of the duct, by multiple loading the duct and, relocating the duct within the magnetic field. In the present paper these later effects were investigated in a duct with an area ratio of 4. The significant results achieved in these experiments were:

1. A 75% increase in power output (from 88 Kw to 153 Kw) was achieved as a result of increasing the duct area ratio.

2. While no shocks indicating choking of the duct were observed in the 2.56 AR duct or for the 10 atm runs of the 4 AR duct. However, shocks were seen to exist in the 4 AR duct at approximately 7 atm and lower. The shock location moved upstream with B-field strength and resulted in a decrease in performance. This indicates that a further increase in performance by increasing the area ratio of the duct may be limited by choking. Thus higher pressure operation may be required to achieve shock-free operation. However, the extent of increased performance at higher pressures is limited by corresponding decreases in electrical conductivity. Preliminary data tends to indicate that the optimum pressure in the present device is $\tilde{\ } \, 10$ atm.

3. For the small duct used in these experiments the gas properties through the duct do not change significantly and hence the majority of the power (95%) can be extracted by a single load. However, the utilization of a second load at the front of the generator did result in a 5% increase in output power.

4. Relocation of the present duct relative to the centerline of the magnet indicated that a small increase in performance could be obtained by moving the duct downstream of its present location. However, the tests indicated that a more optimal utilization of the magnetic field could be obtained with a longer duct. This would allow the use of the full extent of the downstream magnetic field while the upstream region of negative power generation could be made power producing by separately loading the front end and rear regions of the duct.

In experiments now in progress, a duct approximately 25% longer with electrode rings .64 cm thick as compared to the 1.27 cm thickness of the present duct is being tested at area ratios greater than 4.

References

1. Smith, J. M., "Preliminary Results in the NASA Lewis H_2-O_2 Combustion MHD Experiment," Presented at the Proceedings of the 18th Symposium on the Engineering Aspects of Magneto-Hydrodynamics, June 18-20, 1979.

2. Zankl, G., Raeder, J., Dorn, C., and Volk, R., "Experimental Determiniation of Design Data for an MHD Generator," Symposium on the Engineering Aspects of Magnetohydrodynamics, 13th, Stanford University, 1973, pp. II.6.1-II.6.7.

3. Beaton, M. S., Scott, M. H., Wu, Y. C. L., Dicks, J. B., Jr., Muehlkauser, J. W., Holt, W. L., James, H. D., "Insulator Performance and Anode Recession Rate in a Direct Coal Fired Cold Copper Diagonal Conducting Wall MHD Generator," Symposium on the Engineering Aspects of Magnetohydrodynamics, 17th, Stanford University, 1978, pp. D.2.1.-D.2.6.
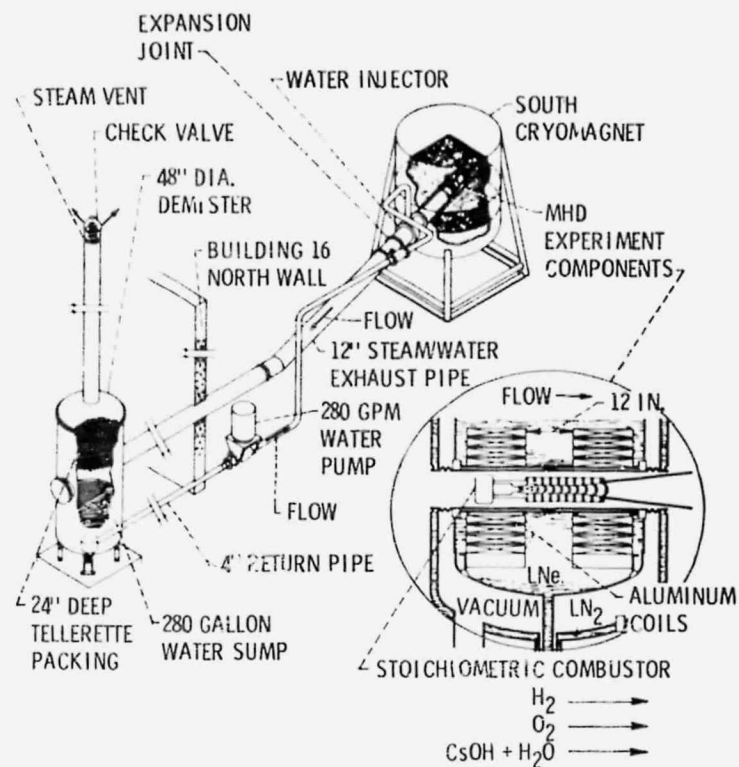
Figure 1. - GH_2-GO_2 combustion MHD experiment installation building 16 room 160.

C-79-684

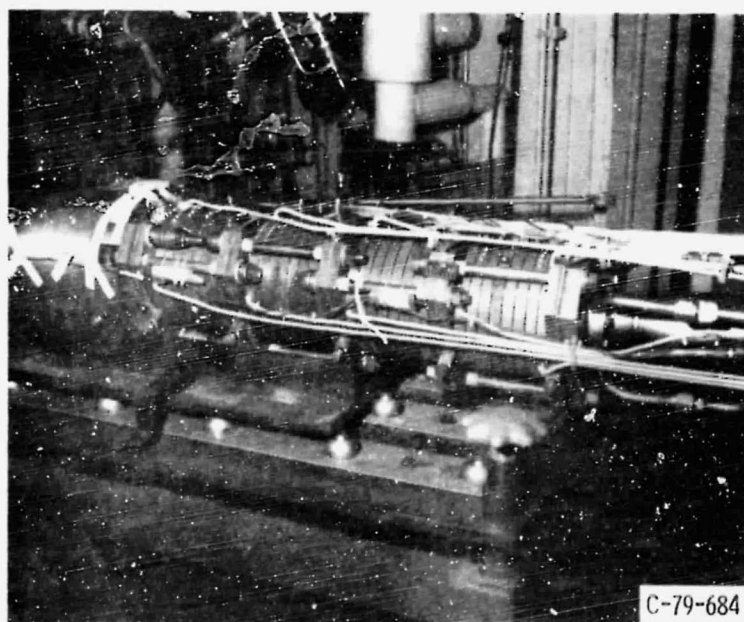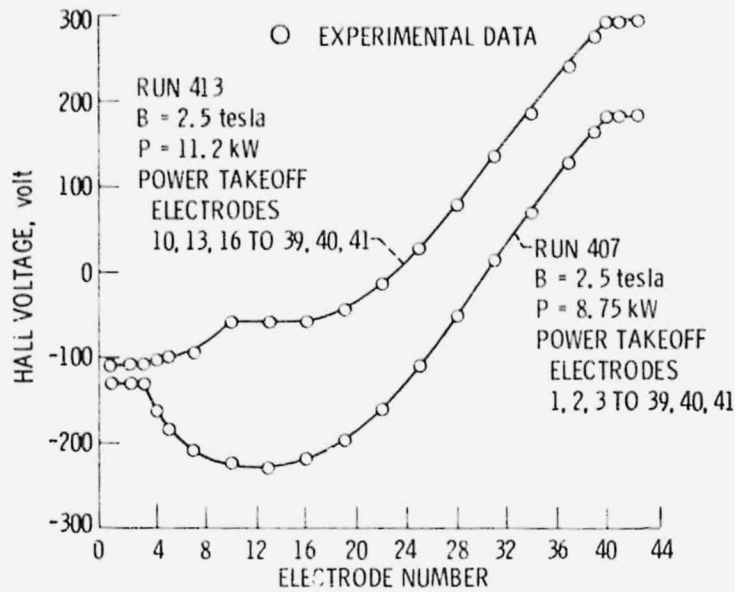Figure 2. - Combustor-generator-diffuser assembly.

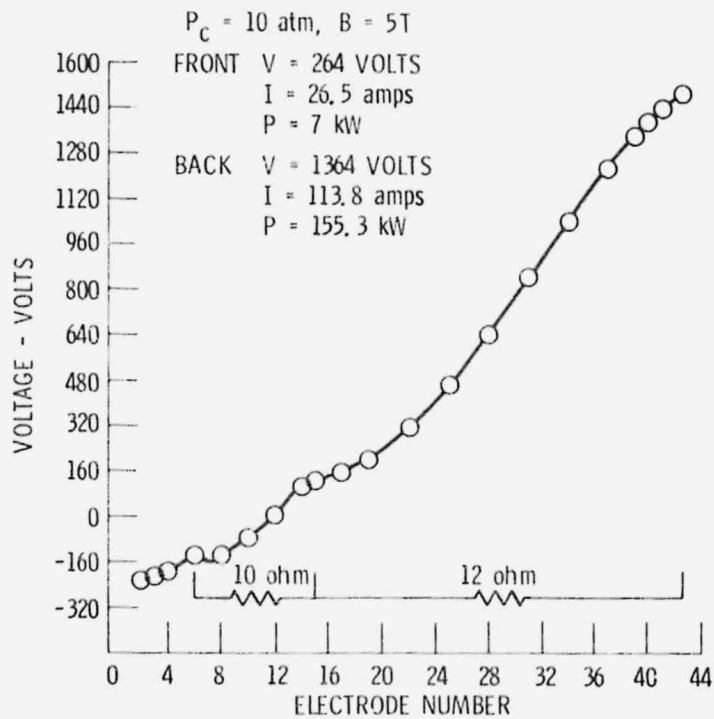Figure 3. - Effect of electrical load on generator performance.

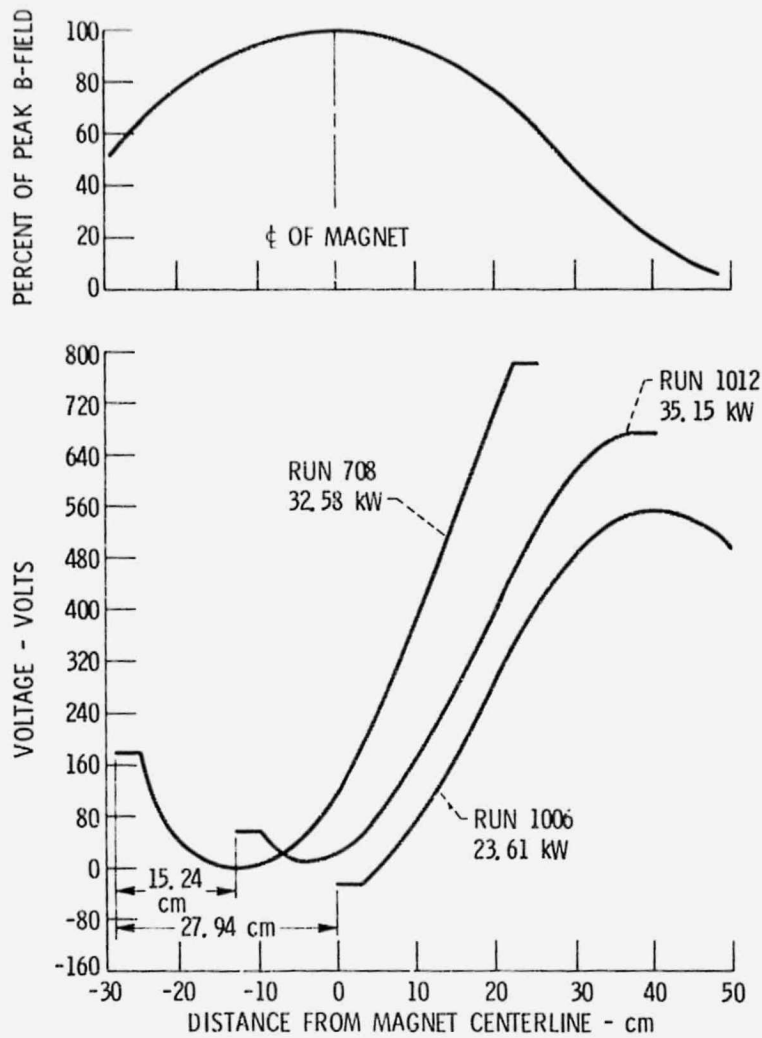Figure 4. - Axial voltage profile for multiple loading.

Figure 5. - Magnet field and voltage distribution in 4 to 1 area ratio duct.
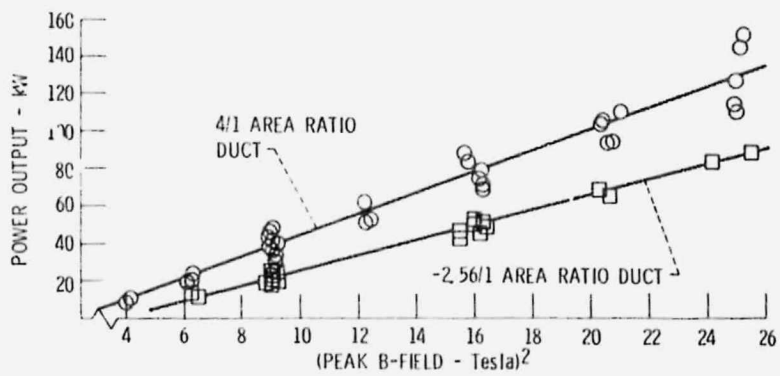

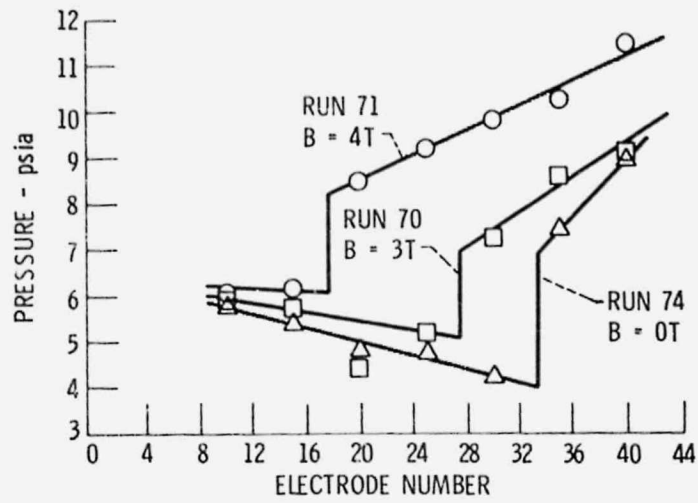Figure 6. - Power output versus B^2 at P_c = 150 psia.

Figure 7. - Axial pressure distribution for various B-fields, combustion pressure of 100 psia.
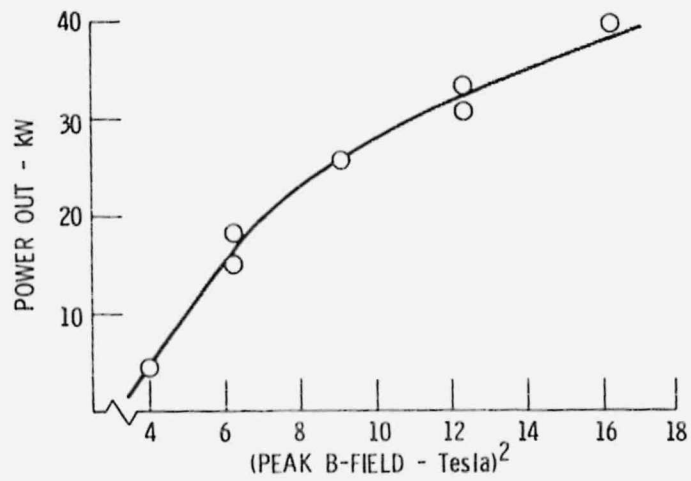
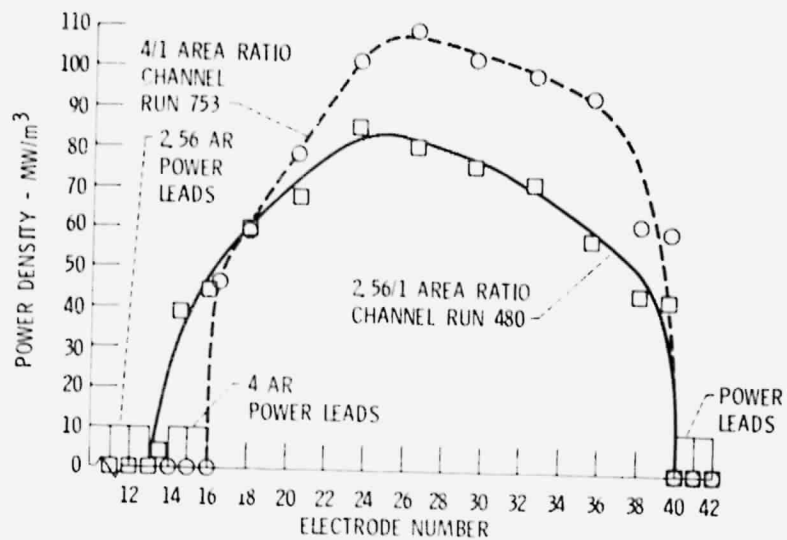Figure 8. - Power output versus B^2 at P_c = 100 psia.

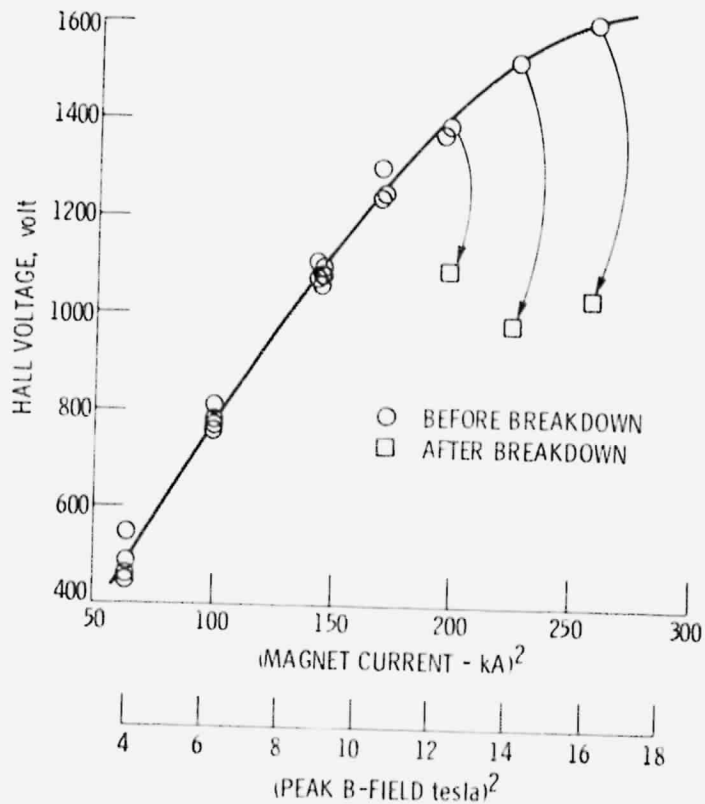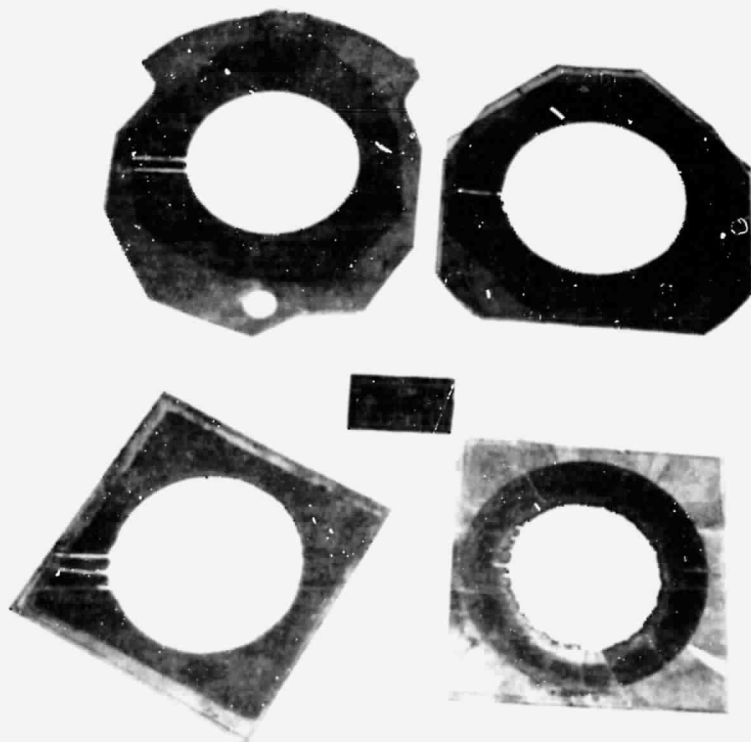Figure 9. - Power density along channel - B = 5 Tesla

Figure 10. - Hall voltage before and after breakdown.

C-79-685

Figure 11. - Interelectrode insulator damage.